Evaluation of microwave plasma oxidation treatments for the fabrication of photoactive un-doped and carbon-doped TiO_2 coatings

Binh H. Q. Dang [1], Mahfujur Rahman [1], Don MacElroy [1], and Denis P. Dowling [1,2,*]

[1] School of Chemical & Bioprocess Engineering, University College Dublin, Ireland

[2] School of Mechanical & Materials Engineering, University College Dublin, Ireland

* Corresponding author,

Dr. Denis P. Dowling

Room 223, UCD Engineering & Materials Science Center,

University College Dublin, Belfield, Dublin 4, Republic of Ireland

Tel: (+353) 1 716 1747

Fax: (+353) 1 283 0534

E-mail: denis.dowling@ucd.ie

Abstract

The photoactivity of both un-doped and carbon-doped titanium dioxide (TiO_2) coatings has been widely reported. In this paper, the use of a microwave plasma as a novel oxidation treatment for the fabrication of these coatings is evaluated. The photoactivity performance of the microwave plasma-formed coatings is benchmarked against those fabricated through air furnace oxidation as well as those deposited using reactive magnetron sputtering. The un-doped and carbon-doped TiO_2 coatings were prepared respectively by microwave plasma-oxidizing titanium metal sheets and sputter deposited titanium carbide thin films. The resulting oxides were characterized using XPS, XRD, FEG-SEM, and optical profilometry. The oxide layer thicknesses achieved over the 15 to 45 minute oxidation times were in the range of 0.15 to 3.44 μm. These coatings were considerably thicker than those obtained by air furnace oxidation. The microwave plasma-formed oxides also exhibited significantly higher surface roughness values compared with the magnetron-sputtered coatings. The photoactivity performance of both un-doped and carbon-doped coatings was assessed using photocurrent density measurements. Comparing the un-doped TiO_2 coatings, it was observed that those obtained using the microwave plasma oxidation route yielded photocurrent density measurements that were 4.3 times higher than the TiO_2 coatings of the same thickness that were deposited by sputtering. The microwave plasma-oxidized titanium carbide coatings did not perform as well as the un-doped TiO_2 probably due to the presence of un-oxidized carbide in the coatings, which reduced their photoactivity.

Keywords: water splitting, sputtering, microwave plasma, titanium oxidation, carbon doping

1. Introduction

Titanium dioxide (TiO_2) thin films have recently found applications in a variety of areas ranging from electrochromics to photocatalysis to photovoltaic solar cells [1-4]. Among the many thin film deposition techniques used, magnetron sputtering in general and DC closed-field magnetron sputtering in particular have been shown to yield coatings exhibiting very good substrate adhesion [5]. This is particularly important for the use of TiO_2 coatings in water-splitting processes for example. One limitation to the magnetron sputtering technique, however, is that without high substrate temperatures, amorphous TiO_2 coatings are generally obtained. Subsequent heat treatments are therefore required to convert the titania coatings into their more photoactive crystalline form. As reported previously, microwave (MW) plasma can be used as a more time- and energy-efficient treatment in alternation to conventional furnace heating for this TiO_2 crystalline conversion [6]. Compared with furnace heat treatments, the MW plasma-treated TiO_2 coatings were also found to possess higher level of surface roughness and hence photoactivity (a 19% increase in photocurrent density measurements) [6]. Nonetheless, the enhanced surface roughness is still only in the order of a few nm and thus the photoactivity of the resulting coatings is relatively limited. The addition of carbon dopants has been found to enhance the photoactivity of sputtered TiO_2 coatings, yet the use of a post-deposition heat treatments generally results in a loss of the dopants [6].

In this study, an alternative fabrication method was investigated to address these two shortcomings. The investigation involved the following microwave plasma treatments:

▪ Microwave plasma oxidation of titanium metal sheets – It has previously been reported that the microarc oxidation of titanium and titanium alloys yields oxide films with high pore density [7].

In this study, microwave plasma oxidation was investigated and a comparison was made with furnace oxidation in air of the same titanium metal substrates.

▪ Microwave plasma oxidation of titanium carbide thin films – It has previously been reported that the direct oxidation of titanium carbide powders significantly increases the surface area [8]. In this study, microwave plasma oxidation of titanium carbide thin films was investigated as a potential route to obtain carbon-doped oxide coatings with increased surface roughness and also enhanced dopant retention.

A further comparison is made with un-doped and carbon-doped TiO_2 coatings deposited using a reactive magnetron sputtering technique [6]. Photocurrent density measurements are used to evaluate the performance for all these coatings as they have been shown to indicate the potential of the coatings for use in water-splitting processes [9, 10].

2. Experimental procedures

2.1. Oxidation of titanium metal sheets – Pure titanium sheets (99.6%, supplied by Goodfellow Cambridge Ltd.) of size 21 × 15 × 0.5 mm^3 were rinsed in a pickling solution (3% HF + 33% HNO_3 + 64% de-ionized H_2O) for 5 min before being ultrasonically cleaned in methanol, followed by acetone for 5 min each. The metal substrates were then plasma-treated in a circumferential antenna plasma (CAP) microwave (2.45 GHz) system, which has been described elsewhere [11]. The chamber was first pumped down to 0.1 mbar at which point 10 sccm of oxygen gas (99.9%) was introduced and the pressure was adjusted to 5 mbar using a manual throttle valve. The microwave discharge was then ignited to form a plasma ball around the samples located in the center of the chamber. Input powers of 2.4 kW were provided from a Mugge microwave power supply. Sample temperatures were measured using a LASCON QP003

two-color pyrometer from Dr. Mergenthaler GmbH & Co. The titanium sheets were treated at 600°C for periods between 15 and 45 min. A parallel study was also carried out with furnace oxidation using a Carbolite CWF 1200 chamber furnace. This box chamber was first heated up to 600°C (ramping 20°C/min) at which point the samples were placed in the furnace for periods between 15 and 45 min and they were then removed.

2.2. Microwave plasma oxidation of magnetron sputter-deposited titanium carbide – The starting point for this study was the deposition of titanium carbide thin films. These were deposited using a Teer Coatings UDP-450 DC closed-field magnetron sputtering system onto the titanium substrates that had been cleaned as described earlier. Pure titanium (99.5%) of size 300 × 100 × 2 mm^3 was used as the sputtering target and distanced 100 mm away from the 2-rpm rotatable substrate holder. Argon (99.998%) was used as the sputtering gas, while methane (99.995%) was used as the reactive gas. Before deposition, the target and the substrates were sputtered cleaned in an argon plasma for 20 min (working pressure of 2×10^{-3} mbar, target current of 0.2 A, and substrate bias voltage of – 400 V). The sputtering condition was then changed to 4×10^{-3} mbar of working pressure, 2 A of target current, and – 50 V of substrate bias voltage before methane was passed in. The methane flow rate was set by a Reactaflo reactive sputtering controller, monitoring the Ti peak, so as to form titanium carbides with different Ti : C ratios (Ti_2C, TiC, and TiC_2). Sputtering time was varied from 30 to 60 min in order to obtain coatings with similar thickness. The resulting thin films were then treated in the microwave oxygen plasma at 600°C for 20 min as detailed earlier.

2.3. Reactive sputter deposition of titanium dioxide coatings – The un-doped and carbon-doped TiO_2 coatings were deposited onto titanium substrates using the same magnetron sputtering conditions as detailed in 2.2. Oxygen was used as the reactive gas for the deposition of

un-doped coatings and the oxygen flow rate was set by the Reactaflo reactive sputtering controller so as to form TiO_2. The deposition time was set to be 25 min to form coatings of approximately 250 nm. Carbon-doped TiO_2 coatings were obtained by introducing carbon dioxide (99.8%) at 4 sccm into the sputtering chamber. The sputtering time was increased to 60 min in order to obtain carbon-doped coatings with the same thickness as the obtained un-doped TiO_2. All the sputtered coatings were then treated in a nitrogen (99.998%) microwave plasma at 700°C for 3 min in order to obtain crystalline conversion [6].

2.4. Characterization techniques – X-ray photoelectron spectroscopy (XPS) analysis of the samples was carried out using a Kratos AXIS 165 spectrometer with a monochromatic Al Kα radiation ($h\nu$ = 1486.58 eV). The degree of crystallinity and the phase composition of the oxidized layers were examined by a Siemens D500 X-ray diffractometer (XRD) operating at 40 kV and 30 mA with Cu Kα radiation at a wavelength of 0.1542 nm. The scan was in 2θ mode and spanned from 20° to 80° with steps of 0.02° per second. The surface morphology of the coatings was visualized using an FEI Quanta 3D FEG-SEM DualBeam system. Surface roughness was measured using a WYKO NT1100 optical profilometer in vertical scanning interferometry (VSI) mode. Photocurrent (I_{ph}) measurements were carried out using a custom-made photo-electrochemical (PEC) cell, a Gamry G300 potentiostat, and a Newport 450W (xenon arc lamp) solar simulator. The PEC cell consisted of three electrodes – the working electrode (TiO_2), the counter electrode (platinum wire), and the reference electrode (saturated calomel electrode – SCE) – all immersed in an electrolyte aqueous solution of 1 M NaOH [6, 10].

3. Results and Discussion

This section is divided into three parts; the first two deals with the characterization of the un-doped and carbon-doped TiO_2 coatings. This is then followed by a study of the photocurrent density measurements of the coatings.

3.1. Oxidized titanium metal sheets – After the microwave plasma oxidation of the titanium metal sheets, the surface appearance changed from metallic to white. The XPS spectra of Ti2p and O1s states for the titanium sheet MW plasma-oxidized for 20 min are given in Fig. 1. The oxidized surface layer is confirmed to be TiO_2 with the expected peaks for Ti^{4+} ($Ti2p_{1/2}$ at 458.5 eV and $Ti2p_{3/2}$ at 464.2 eV) and O^{2-} (529.7 eV – The peak at 531.3 eV is due to surface hydroxyl groups) exhibited in the spectra [12-15]. Similar peaks were observed for all oxidized titanium surfaces.

Fig. 2a plots the evolution with time of the XRD patterns for the MW plasma-oxidized titanium sheets. It further illustrates that the resulting titanium dioxide layers are a mixed phase of TiO_2 rutile and anatase, with rutile being the primary component. Using the equation $f_R = 1 / [1 + (0.884I_A/I_R)]$ by Spurr and Myers [16] where I_A and I_R represent the integral intensities of the strongest anatase peak (in this case A(103)) and the strongest rutile peak (either R(110) or R(101)) respectively, the mass fraction of rutile (f_R) in the titanium sheets MW plasma-oxidized for 15 to 45 min was estimated to range from 77 to 92%. Furnace-oxidized titanium sheets exhibited mixed-phase composition for the sample treated for 15 min ($f_R \approx 77\%$) but those treated for longer times are of pure rutile phase only (Fig. 2b). It should also be noted that the crystalline growth with time for (110)-oriented rutile is much faster for the microwave plasma oxidation route than obtained using furnace oxidation.

Fig. 3a illustrates the oxidation growth for the MW plasma-oxidized samples based on the change in the oxide surface layer thickness with variation in oxidation time from 15 to 45 min. Oxide thickness was determined by gravimetric analysis as $\frac{\Delta w}{d \times A}$ [17] with Δw being the weight difference between pre- and post-oxidation whereas A is the area of the sheets (3.15 cm^2) and d is the density of rutile TiO_2 (4.25 g/cm^3), which is the primary phase of the resulting oxides as established earlier through XRD. This gravimetric analysis is based on the observation that the weight gain Δw is mainly attributed to TiO_2 formation since Δw was not detected for microwave-induced argon plasma treatments. The thickness values given in Fig. 3a were confirmed for selected coatings based on FEG-SEM cross-sectional analysis data (Fig. 3b). The TiO_2 coating thickness data demonstrate an initial slow increase in oxide layer thickness, but for microwave plasma oxidation longer than 30 min there is a relatively rapid increase. This latter increased rate of oxidation may be a result of an increase in the coating porosity or a thermal breakdown of the oxide layer after long treatment times, either of which would facilitate more oxygen absorption and hence a more rapid rate of oxidation. The same trend was found for furnace-oxidized titanium sheets yet the oxide surface layer thicknesses were only one-quarter of those fabricated through microwave plasma oxidation (Fig. 3a). A factor influencing the significantly decreased rate of oxidation in the furnace compared with the microwave plasma is the presence of ~ 21% oxygen in air, whereas the microwave plasma oxidation was carried out in an oxygen-only plasma. This conclusion is supported by the observation by Kakizaka et al. that oxidation rate is directly proportional to the number density of oxygen atoms [18].

3.2. Microwave plasma-oxidized titanium carbide – For this study, the sputtered titanium carbide coatings were oxidized as before using the microwave oxygen plasma. The resulting oxide surface layers were again determined by XPS and XRD to be crystalline TiO_2 of mixed

phase, with rutile being the primary component. The presence of carbon dopants was verified by the deconvoluted XPS spectra of C1s states in Fig. 4a. The peak at 282.8 eV is assigned to doped carbon O–Ti–**C,** whereas the peak at 281.7 eV represents non-dopant carbide carbon Ti–**C** from the starting material [19, 20]. With increasing Ti : C ratio in the starting Ti_xC_y coating, the level of titanium oxidation will increase and this may explain the chemical shift of the Ti–**C** peaks in Fig. 4a. This shift towards the O–Ti–**C** peaks is likely to be due to an increased number of oxidized titanium species in the lattice (TiC_2 < TiC < Ti_2C as shown in Fig. 4b). Additionally, the degree of conversion from non-dopant Ti–**C** carbons to doped O–Ti–**C** carbons is dependent on the degree of titanium oxidation. As a result, the percentage of doped O–Ti–**C** carbons in the oxidized Ti_xC_y is found to increase with increasing titanium content (decreasing carbon content) in Ti_xC_y from 1.6% (TiC_2) to 2.3% (TiC) to 2.4% (Ti_2C) as shown in Fig. 4c.

3.3. Photocurrent density measurements – The photocurrent densities obtained after furnace oxidation or microwave plasma oxidation of titanium metal sheets for 20 min are given in Fig. 5. At ~ 0.23 V versus SCE (1.23 V versus RHE) which is the minimum theoretical voltage required to split water [1], the photocurrent density measured for TiO_2 fabricated through microwave plasma oxidation is 1.8 times higher than that produced through furnace oxidation (908 vs. 494 $\mu A/cm^2$). This enhanced performance can be explained for by the earlier observation that, for similar oxidizing time and temperature, the MW plasma-formed TiO_2 layer is four times thicker than obtained through furnace oxidation. Additionally, whereas furnace oxidation resulted in coatings of pure rutile with a higher percentage of R(101), microwave plasma oxidation resulted in coatings of mixed phase with a higher percentage of (110)-oriented rutile. Coatings of mixed phased TiO_2 in general have been found in the literature to have better performance than

those of pure phases alone [19, 21, 22] and R(110) has also been shown to be the more stable photoactive crystal face of rutile [23, 24].

A comparison was made between the titanium sheet MW plasma-oxidized for 20 min and the magnetron-sputtered TiO_2 coating with the same thickness (~ 250 nm). As demonstrated in Fig. 5, there is a 4.3-fold enhancement in photocurrent density for the MW plasma-formed oxide layer (908 vs. 213 $\mu A/cm^2$). This improvement can be accounted for by the much rougher surface obtained after microwave plasma oxidation (Fig. 6). A further contributory factor is that the TiO_2 coating produced from this oxidation route is of mixed phase rather than the pure anatase form which is obtained in the case of the sputtered TiO_2 after thermal treatment [6]. ~~Coatings of mixed-phase TiO_2 in general have been found in the literature to have better performance than those of pure phases alone [19, 21, 22].~~

The effect of carbon-doping is evaluated as shown in Fig. 7 which plots the photocurrent density measurements for the MW plasma-oxidized Ti_xC_y thin films. At ~ 0.23 V, the photocurrent density measured for the oxidized Ti_2C coating (433 $\mu A/cm^2$) is 19% higher than that obtained from the oxidized TiC coating (365 $\mu A/cm^2$) and is 37% higher than that for the oxidized TiC_2 coating (317 $\mu A/cm^2$). It was concluded from this study that the higher the doped O-Ti-**C** carbon content, the higher the photocurrent density produced. In comparison to the carbon-doped TiO_2 coating deposited by magnetron sputtering with photocurrent density measurement of 275 $\mu A/cm^2$, the corresponding values obtained for the MW plasma-oxidized Ti_xC_y were all found to be significantly higher. While a major factor is the increased roughness of the MW plasma-oxidized surfaces, a contributory factor is also likely to be the retention of higher levels of doped O-Ti-**C** carbons. As shown previously, the use of heat treatments following sputtering significantly reduced the carbon dopant content [6].

Carbon-doping has been reported to enhance the photoactivity of TiO_2 [8, 9, 25]. This is supported by the observation made earlier about higher dopant content resulting in higher photocurrent density. Nevertheless, when Fig. 5 and 7 are compared, it is clear that the photocurrent density produced by MW plasma-oxidized titanium metal sheet, i.e. un-doped TiO_2, is much higher than that produced by MW plasma-oxidized titanium carbide thin film, i.e. carbon-doped TiO_2 (908 vs. 433 $\mu A/cm^2$). A possible explanation for this is the presence of a relatively high level of the non-dopant Ti–**C** carbide carbons in the latter coating as demonstrated by XPS. A summary of all the photocurrent density measurements is given in Table 1.

4. Conclusions

This study has demonstrated that the use of microwave plasma oxidation of titanium has been found to yield oxide layers that exhibit higher levels of photoactivity, particularly when compared with TiO_2 coatings (with the same thickness) deposited by reactive magnetron sputtering. The enhanced performance is due to the significantly improved surface roughness of the MW plasma-formed oxide. Furnace oxidation at the same temperature for the same time periods as used in the microwave plasma oxidation yielded oxide layer thicknesses of only one-quarter of those obtained through the microwave plasma oxidation route. A comparison of performance based on photocurrent density measurements demonstrated that the microwave plasma oxidation route yielded coatings with enhanced photocurrent density as compared to the furnace oxidation (1.8-fold enhancement) and magnetron sputtering deposition (4.3-fold).

Carbon-doped TiO_2 coatings were obtained by the microwave plasma oxidation of sputtered titanium carbide thin films. This study demonstrated that with lower carbon concentration in the starting titanium carbide (i.e. Ti_2C), the resulting MW plasma-formed

carbon-doped coating exhibited higher photocurrent densities. This is likely to be due to higher content of carbon dopants in the coating. While all of these MW plasma-formed carbon-doped coatings exhibited better photoactivity than sputtered carbon-doped TiO_2, they unexpectedly exhibited poorer performance to the un-doped MW plasma-formed TiO_2. The retention of non-dopant Ti–**C** carbons in the doped coatings is a likely explanation for this. In conclusion, microwave plasma oxidation has potential as a processing technology for the fabrication of photoactive TiO_2 coatings.

Acknowledgments

The authors wish to acknowledge the grant of Science Foundation Ireland for funding this work through the Strategic Research Cluster on Solar Energy Conversion (Project No. 07/SRC/B1160).

References

[1] A. Fujishima, K. Honda, Nature, 238 (1972) 37-+.
[2] A. Fujishima, X.T. Zhang, D.A. Tryk, Surface Science Reports, 63 (2008) 515-582.
[3] O. Khaselev, J.A. Turner, Science, 280 (1998) 425-427.
[4] X. Chen, S.S. Mao, Chemical Reviews, 107 (2007) 2891-2959.
[5] S. Swann, Physics in Technology, 19 (1988) 67-75.
[6] B.H.Q. Dang, M. Rahman, D. MacElroy, D.P. Dowling, Surface & Coatings Technology, 205 (2011) S235-S240.
[7] Y.K. Shin, W.S. Chae, Y.W. Song, Y.M. Sung, Electrochem Commun, 8 (2006) 465-470.
[8] M. Shen, Z.Y. Wu, H. Huang, Y.K. Du, Z.G. Zou, P. Yang, Mater Lett, 60 (2006) 693-697.
[9] S.U.M. Khan, M. Al-Shahry, W.B. Ingler, Science, 297 (2002) 2243-2245.
[10] M. Rahman, J.M.D. MacElroy, D.P. Dowling, Journal of Nanoscience and Nanotechnology, 11 (2011) 8642-8651.
[11] M.L. McConnell, D.P. Dowling, C. Pope, K. Donnelly, A.G. Ryder, G.M. O'Connor, Diamond and Related Materials, 11 (2002) 1036-1040.
[12] F. Werfel, O. Brummer, Phys Scripta, 28 (1983) 92-96.
[13] S.O. Saied, J.L. Sullivan, T. Choudhury, C.G. Pearce, Vacuum, 38 (1988) 917-922.
[14] Z.L. Liu, L. Hong, B. Guo, J Power Sources, 143 (2005) 231-235.
[15] Z. Lin, I.S. Lee, Y.J. Choi, I.S. Noh, S.M. Chung, Biomed Mater, 4 (2009).
[16] R.A. Spurr, H. Myers, Analytical Chemistry, 29 (1957) 760-762.
[17] J. Krysa, M. Zlamal, G. Waldner, J Appl Electrochem, 37 (2007) 1313-1319.

[18] S. Kakizaka, T. Sakamoto, H. Matsuura, H. Akatsuka, J Adv Oxid Technol, 10 (2007) 253-259.
[19] F. Dong, H.Q. Wang, Z.B. Wu, Journal of Physical Chemistry C, 113 (2009) 16717-16723.
[20] E. Lewin, K. Buchholt, J. Lu, L. Hultman, A.L. Spetz, U. Jansson, Thin Solid Films, 518 (2010) 5104-5109.
[21] P.W. Chou, S. Treschev, P.H. Chung, C.L. Cheng, Y.H. Tseng, Y.J. Chen, M.S. Wong, Applied Physics Letters, 89 (2006) -.
[22] A. Testino, I.R. Bellobono, V. Buscaglia, C. Canevali, M. D'Arienzo, S. Polizzi, R. Scotti, F. Morazzoni, Journal of the American Chemical Society, 129 (2007) 3564-3575.
[23] D. Ulrike, Chapter 11 The structure of TiO2 surfaces, in: D.P. Woodruff (Ed.) The Chemical Physics of Solid Surfaces, Elsevier, 2001, pp. 443-484.
[24] T.Y. Ke, C.W. Peng, C.Y. Lee, H.T. Chiu, H.S. Sheu, Crystengcomm, 11 (2009) 1691-1695.
[25] H. Irie, Y. Watanabe, K. Hashimoto, Chemistry Letters, 32 (2003) 772-773.

Tables

Table 1. Comparison of un-doped and C-doped TiO_2 coatings fabricated through magnetron sputtering and direct furnace / MW plasma oxidation pathways.

	Un-doped TiO_2	**C-doped TiO_2**
▪ **Magnetron sputtering**		
- As-deposited	108 μA/cm^2	138 μA/cm^2
- MW plasma thermally treated	213 μA/cm^2	275 μA/cm^2
▪ **Direct oxidation**		
- Furnace oxidation	494 μA/cm^2	311 μA/cm^2
- MW plasma oxidation	908 μA/cm^2	433 μA/cm^2

Figure captions

Fig. 1: XPS spectra of (a) Ti2p state and (b) O1s state for the titanium sheet which had been MW plasma-oxidized for 20 min.

Fig. 2: Evolution of the XRD patterns for (a) the MW plasma-oxidized and (b) the furnace-oxidized titanium sheets.

Fig. 3: (a) Change in the oxide surface layer thickness with variation in oxidation time; (b) Cross section of the titanium sheet which had been MW plasma-oxidized for 45 min.

Fig. 4: (a) Deconvoluted XPS spectra of C1s state for the MW plasma-oxidized Ti_xC_y thin films; (b) Deconvoluted XPS spectra of Ti2p state for the MW plasma-oxidized Ti_xC_y thin films; (c) The influence of carbon concentration in the original Ti_xC_y coating on the resulting carbon dopant content.

Fig. 5: Photocurrent density measurements for the MW plasma-oxidized, furnace-oxidized, and magnetron-sputtered TiO_2.

Fig. 6: Surface morphology of (a) Heat-treated sputtered TiO_2 and (b) MW plasma-oxidized titanium sheet.

Fig. 7: Photocurrent density measurements for the MW plasma-oxidized (MWPO) Ti_xC_y thin films and the magnetron-sputtered carbon-doped TiO_2 coating.

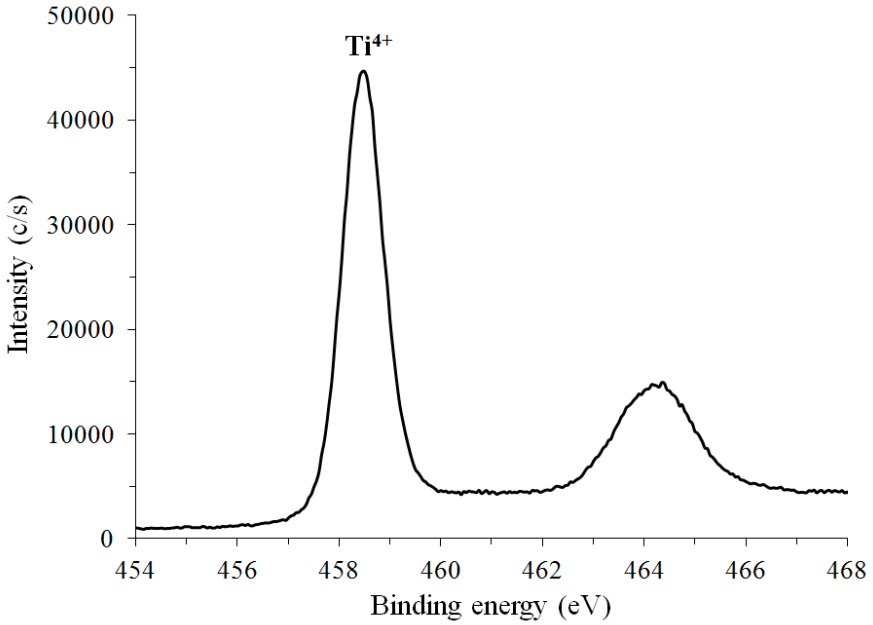
Ti4+
Intensity (c/s)
50000
40000
30000
20000
10000
0
454
456
458
460
462
464
466
468
Binding energy (eV)

(a)

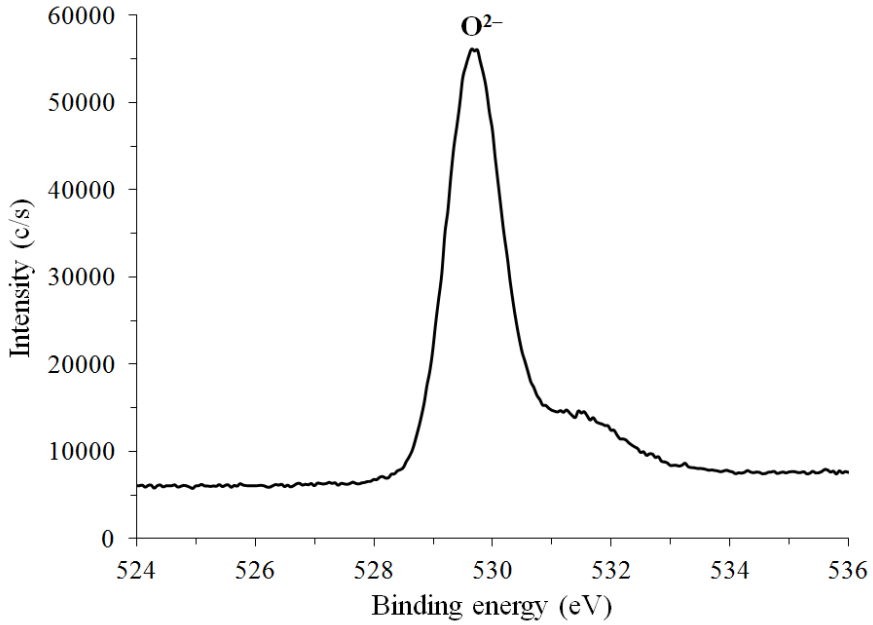
O2–
Intensity (c/s)
60000
50000
40000
30000
20000
10000
0
524
526
528
530
532
534
536
Binding energy (eV)

(b)

Fig. 1

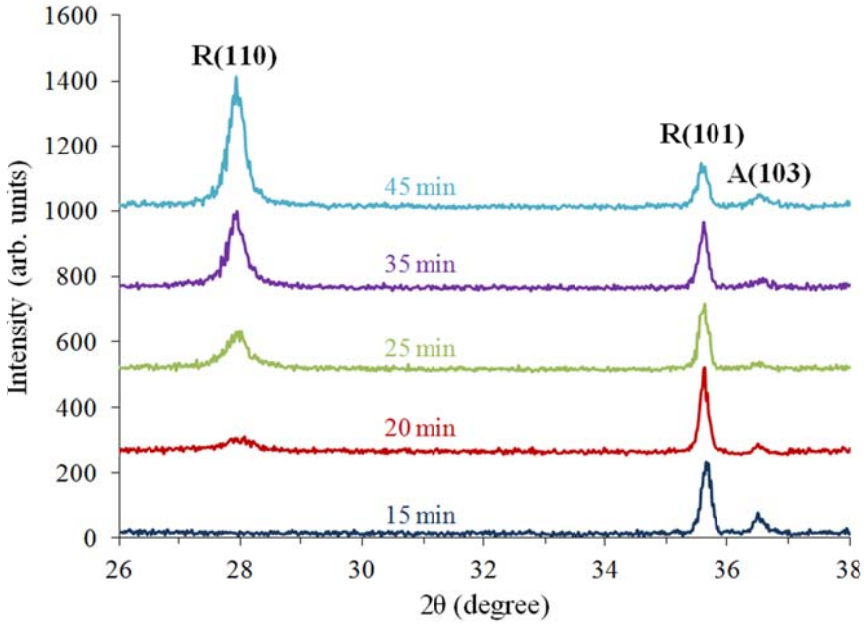
R(110)
R(101)
A(103)
45 min
35 min
25 min
20 min
15 min
Intensity (arb. units)
2θ (degree)
1600
1400
1200
1000
800
600
400
200
0
26
28
30
32
34
36
38

(a)

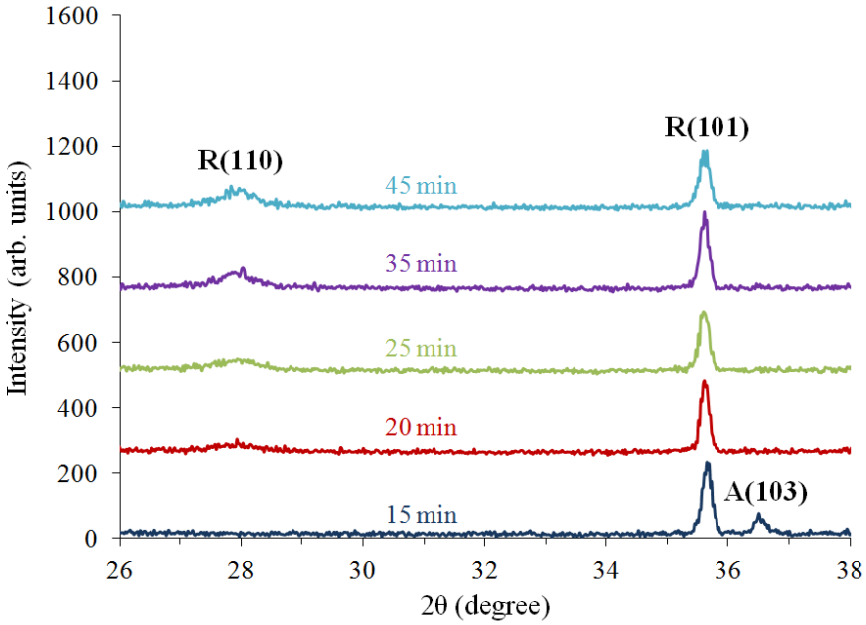
R(110)
R(101)
A(103)
45 min
35 min
25 min
20 min
15 min
Intensity (arb. units)
2θ (degree)
1600
1400
1200
1000
800
600
400
200
0
26
28
30
32
34
36
38

(b)

Fig. 2

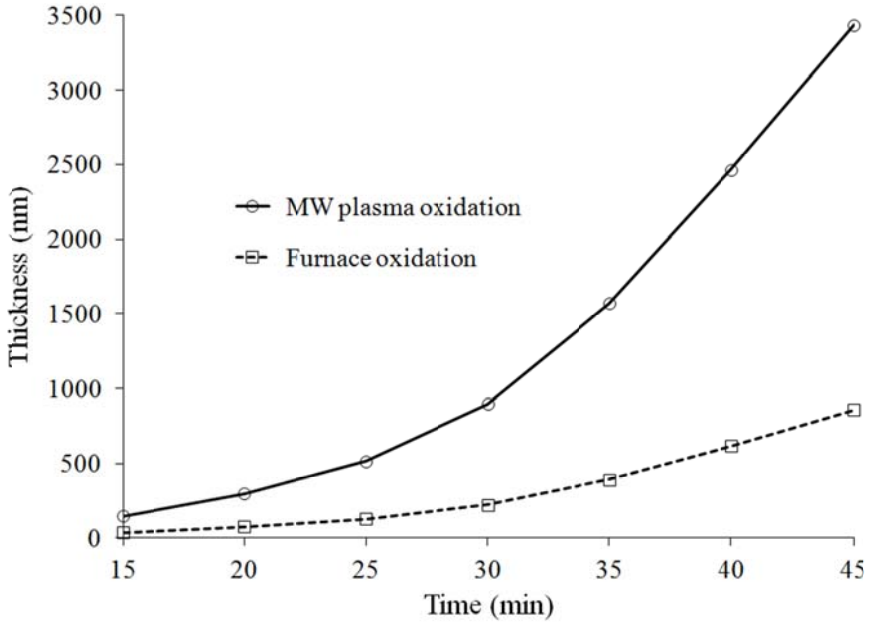
3500
3000
2500
2000
1500
1000
500
0
Thickness (nm)
MW plasma oxidation
Furnace oxidation
15
20
25
30
35
40
45
Time (min)

(a)

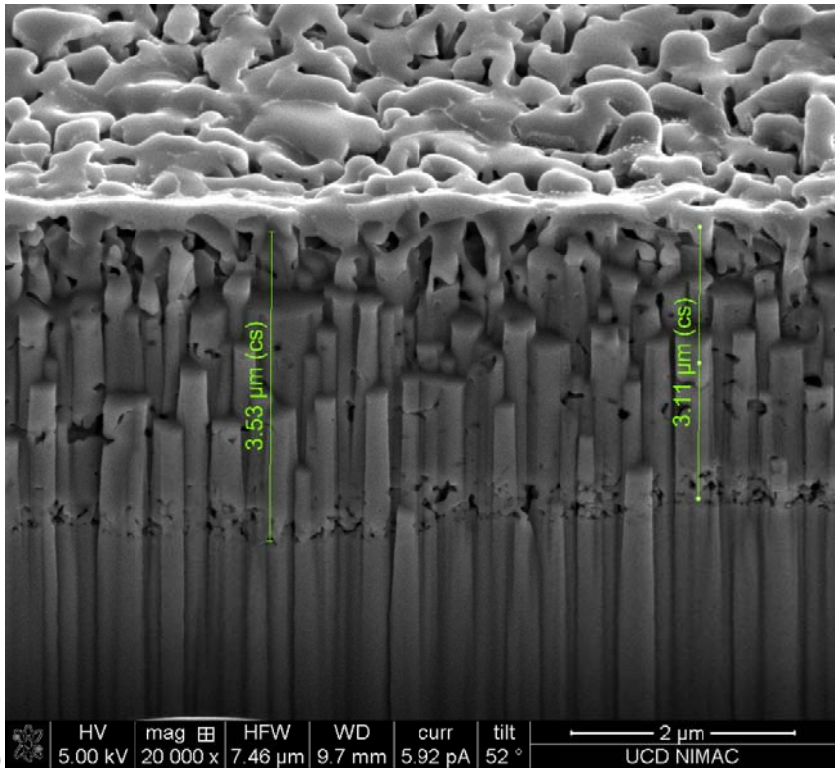
3.53 µm (cs)
3.11 µm (cs)
HV
5.00 kV
mag
20 000 x
HFW
7.46 µm
WD
9.7 mm
curr
5.92 pA
tilt
52 °
2 µm
UCD NIMAC

(b)

Fig. 3

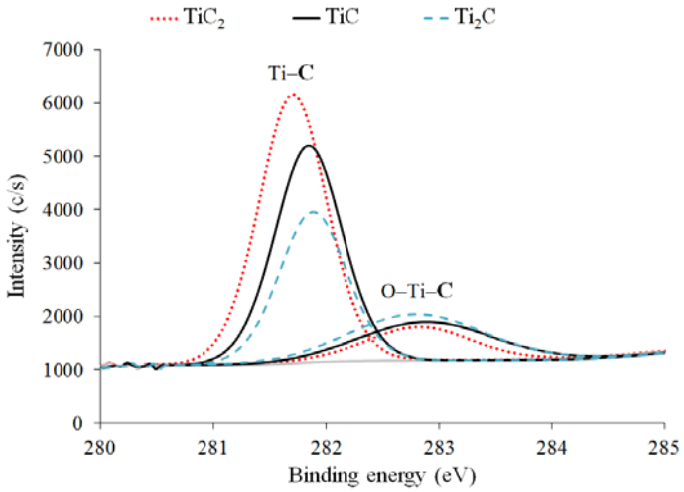
TiC2
TiC
Ti2C
Ti–C
O–Ti–C
Intensity (c/s)
Binding energy (eV)

(a)

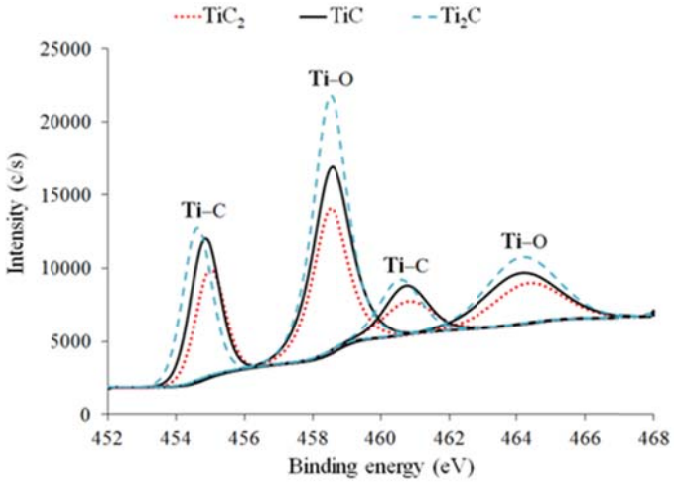
TiC2
TiC
Ti2C
Ti–O
Ti–C
Ti–C
Ti–O
Intensity (c/s)
Binding energy (eV)

(b)

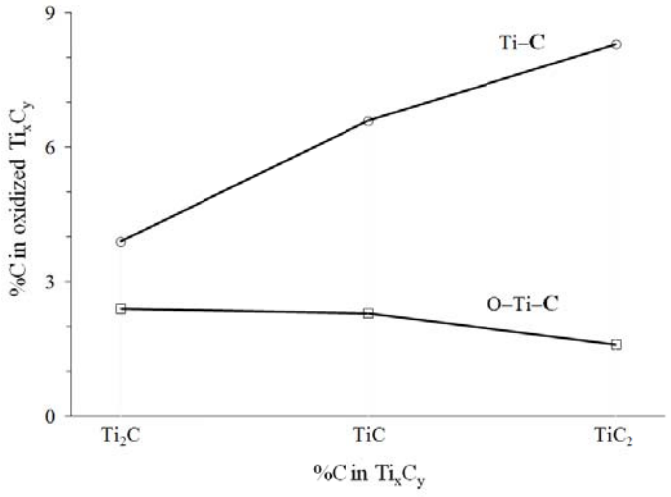
Ti–C
O–Ti–C
%C in oxidized TixCy
Ti2C
TiC
TiC2
%C in TixCy

(c)

Fig. 4

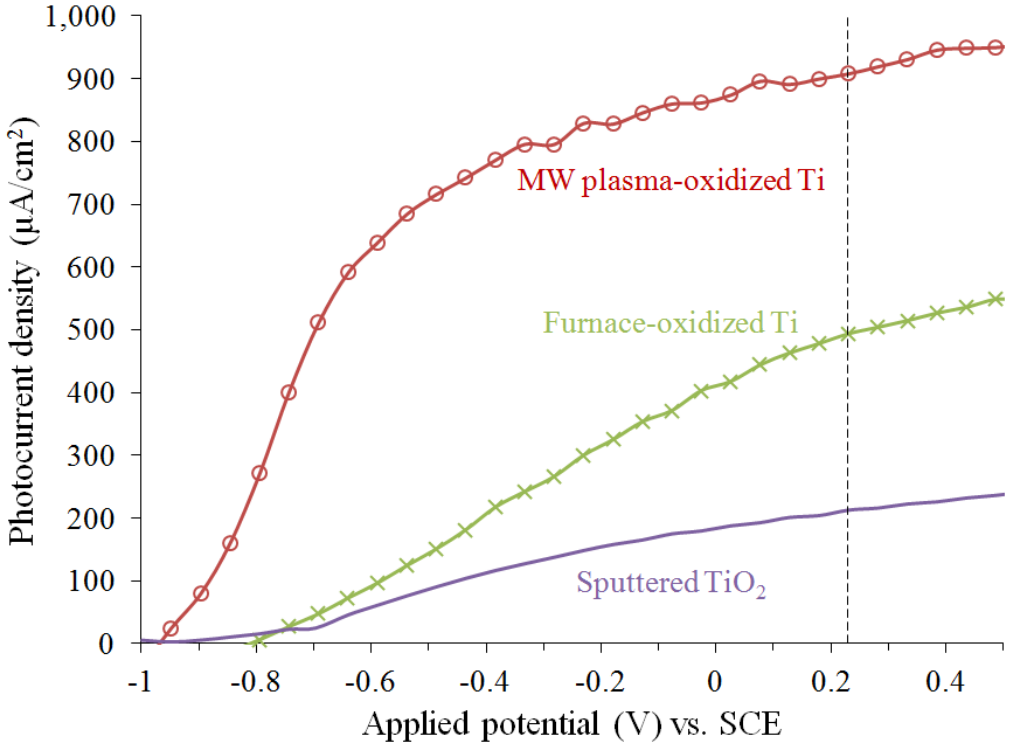
1,000
900
800
700
600
500
400
300
200
100
0
Photocurrent density (μA/cm²)
MW plasma-oxidized Ti
Furnace-oxidized Ti
Sputtered TiO2
-1
-0.8
-0.6
-0.4
-0.2
0
0.2
0.4
Applied potential (V) vs. SCE

Fig. 5

(a)

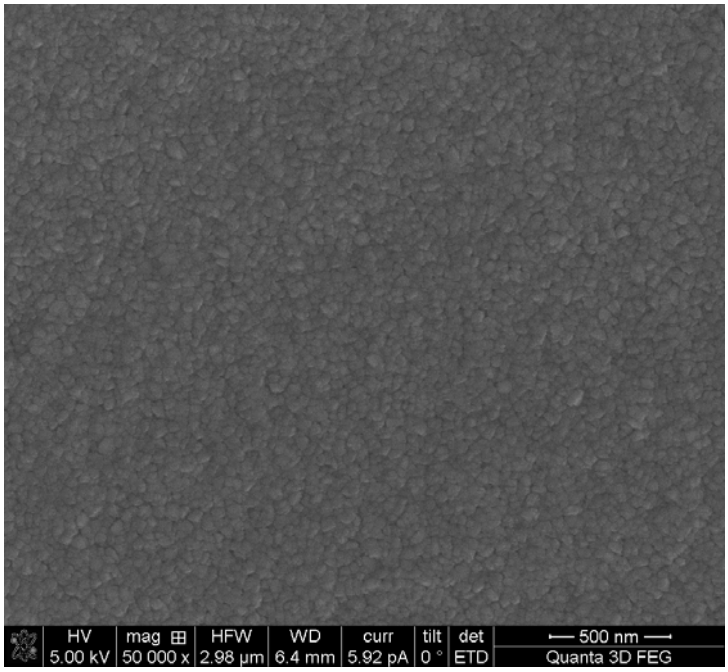
HV
5.00 kV
mag
50 000 x
HFW
2.98 µm
WD
6.4 mm
curr
5.92 pA
tilt
0 °
det
ETD
500 nm
Quanta 3D FEG

(b)

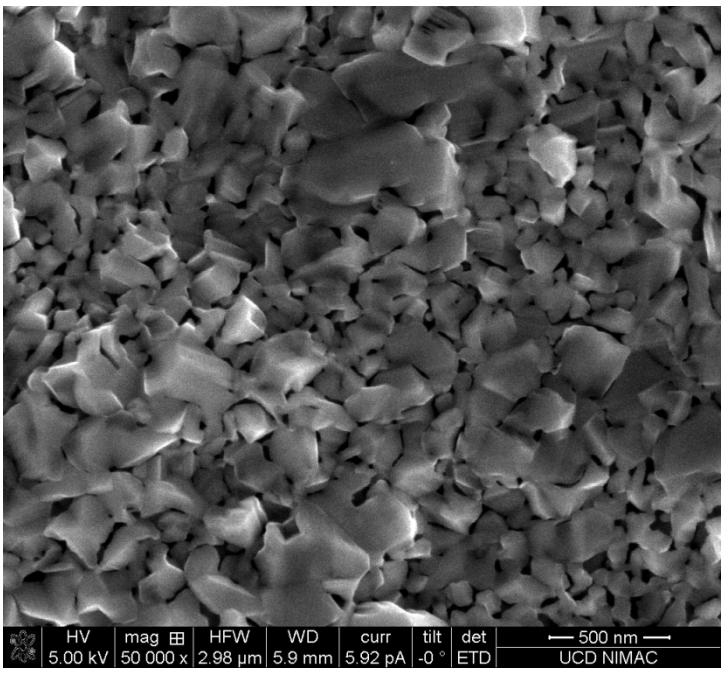
HV
5.00 kV
mag
50 000 x
HFW
2.98 µm
WD
5.9 mm
curr
5.92 pA
tilt
-0 °
det
ETD
500 nm
UCD NIMAC

Fig. 6

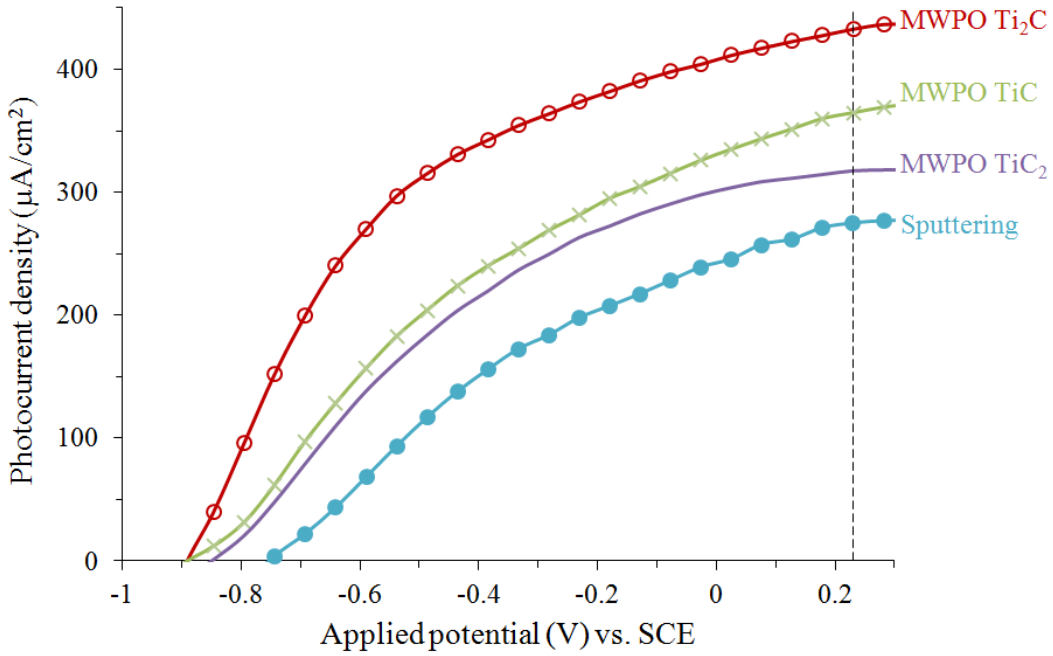
MWPO Ti_2C
MWPO TiC
MWPO TiC_2
Sputtering
Photocurrent density (μA/cm²)
400
300
200
100
0
-1
-0.8
-0.6
-0.4
-0.2
0
0.2
Applied potential (V) vs. SCE

Fig. 7